Journal of Materials Chemistry B

PAPER

View Article Online
View Journal | View Issue

Cite this: J. Mater. Chem. B, 2014, 2, 3490

LHRH-peptide conjugated dextran nanoparticles for targeted delivery of cisplatin to breast cancer

Mingqiang Li,[ac] Zhaohui Tang,[a] Yu Zhang,[ac] Shixian Lv,[ac] Haiyang Yu,[a] Dawei Zhang,[a] Hua Hong[b] and Xuesi Chen*[a]

Cisplatin is one of the most common anticancer agents for treating different kinds of solid tumors today. However, its broader therapeutic applications are limited by the severe side effects and nonspecific biodistribution. In this study, luteinizing hormone-releasing hormone (LHRH)-targeted polysaccharide nanoparticles for tumor-targeted delivery and controlled release of cisplatin were developed. This nanoparticle delivery system possessed the following unique properties: (1) as the degradation products of the carrier, both dextran and succinic acid have been proved by the United States Food and Drug Administration for parenteral use, indicating good safety and great application potential; (2) both the drug loading and LHRH conjugation procedures were carried out with efficiency in aqueous medium without the use of organic solvents, thus representing a green chemistry approach; and (3) the design followed the principle of drug encapsulation first and subsequent targeting ligand modification, guaranteeing that the targeting molecules were conjugated on the surface of nanoparticles. As compared to free cisplatin, both the non-targeted and targeted nanoparticles displayed sustained drug release, prolonged blood circulation and reduced systemic toxicity. Foremost, the LHRH-targeted nanoparticles led to significant higher cellular internalization in MCF-7 tumor cells *in vitro* and enhanced accumulation in MCF-7 xenograft tumors *in vivo*, compared with the non-targeted counterparts. Systemic delivery of the targeted nanoparticles carrying cisplatin *via* intravenous injection showed enhanced tumor suppression in MCF-7 tumor bearing mice compared to the non-targeted nanoparticles and free CDDP. Collectively, the LHRH-mediated polysaccharide nanoparticles appeared to be a promising nanomedicine drug delivery system for tumor-targeted delivery of cisplatin.

Received 13th January 2014
Accepted 29th March 2014

DOI: 10.1039/c4tb00077c

www.rsc.org/MaterialsB

Introduction

With one in nine women developing breast cancer during their lifetime, breast cancer is the most common cancer in women worldwide accounting for 23% of the total cancer cases.[1,2] Despite great efforts in its diagnosis and treatment, breast cancer remains a leading cause of cancer-related deaths among women,[3] representing 14% of the global cancer deaths.[2] It is estimated that, in 2012, there were more than 39 000 deaths due to breast cancer in the United States alone.[3] Therefore, it is urgent to develop new agents and treatment strategies for breast cancer.

cis-Diamminedichloroplatinum (cisplatin, CDDP), one of the most common anticancer agents, has been used in the treatment of different kinds of solid tumors including breast, ovarian, head and neck, gastrointestinal, testicular, bladder, and lung cancers.[4,5] Nearly 50% of all chemotherapeutic regimens administered to patients include CDDP.[6] However, the broader therapeutic applications of CDDP are limited by its severe side effects, such as nephrotoxicity, peripheral neuropathy, nausea, anemia and ototoxicity, which may result from its nonspecific systemic organ distribution and inadequate intratumor concentration.[7]

Compared to the conventional chemotherapeutic agents, nano-scaled polymeric drug delivery systems for cancer therapy have demonstrated many distinct advantages, including versatile physicochemical properties, improved drug solubility, prolonged circulation time through avoiding rapid clearance by the renal and reticuloendothelial systems (RES), decreased side effects, passive targeting of tumor tissues *via* the enhanced permeability and retention (EPR) effect, and improved drug bioavailability.[8,9] By encapsulating or incorporating CDDP in nano-scaled carriers, such as long-circulating liposomes,[10,11] dendrimers,[12] polysaccharides,[7,13] and synthetic polymer micelles,[14,15] tumor-targetable cisplatin formulations *via* an EPR guided strategy were formed. Favored biodistribution and much lower side effects were proved. NC-6004, a cisplatin-incorporated micellar formulation developed by Kataoka *et al.*, has

[a]Key Laboratory of Polymer Ecomaterials, Changchun Institute of Applied Chemistry, Chinese Academy of Sciences, Changchun 130022, P.R. China. E-mail: xschen@ciac.ac.cn; Fax: +86 431 85262112; Tel: +86 431 85262112
[b]Laboratory Animal Center, Jilin University, Changchun, 130012, P.R. China
[c]University of Chinese Academy of Sciences, Beijing 100049, P.R. China

been demonstrated to show a remarkably high drug loading content and low systemic toxicity, which have already been tested in phase-I/II clinical trials.[16–18] Recently, platinum(IV) prodrugs, which are inert and will not undergo hydrolysis or ligand substitutions in the blood but will be activated in cells by reductive elimination, are also widely studied.[19–23]

In addition to reducing the overall toxicity and altering biodistribution *via* the EPR effect, further increasing the tumor accumulation of anti-cancer drugs *via* active targeting ligands also plays an important role in clinical cancer therapy. Compared with the non-targeted nanoparticles, the tumor-targeted nanoparticles can enter tumor cells *via* receptor-mediated internalization, with the potential to significantly reduce toxicity and improve its therapeutic performance.[7] For this specific reason, various tumor targeting ligands, such as antibodies, proteins, peptides, aptamers and small molecules, have been used to facilitate the internalization of nanoparticles into target cells.[24] Shin *et al.* developed EGFR-targeted nanoparticles, which led to significantly higher accumulation of CDDP in tumor cells and the enhanced antitumor effect both *in vitro* and *in vivo*, while significantly reducing the toxicity of CDDP to the spleen and kidney.[7] Recently, Kataoka and co-workers achieved highly efficient drug delivery to glioblastoma (U87MG) by using a platinum anticancer drug-incorporating polymeric micelle with cyclic Arg–Gly–Asp (cRGD) ligand molecules.[25] Our previous study proved that a combination of CDDP-loaded poly(ethylene glycol)-*b*-poly(L-glutamic acid) nanoparticles and iRGD could significantly reduce the toxicity and increase the tumor accumulation of CDDP.[26] Despite these burgeoning developments, effective methods for facile synthesis of the simple, efficient and safe tumor-targeted nanoparticles for the selective delivery of CDDP are still much in demand.

Overexpression of the luteinizing hormone-releasing hormone (LHRH) receptors has been found in many tumors including ovarian and endometrial (about 80%), prostate (about 90%), and breast (about 50%) tumors, while their expression is scarce in healthy tissues, which makes them an ideal tumor target for constructing nanoparticles for targeted therapy of gonadal tumors.[27–29] Several studies have reported targeting the LHRH-receptor positive neoplasm utilizing the analogues of LHRH peptides. However, most of these studies focused on delivery of hydrophobic anticancer drugs (camptothecin, paclitaxel, methotrexate, *etc.*).[30–32] Recently, Bronich and co-workers have reported the first example of LHRH-targeted CDDP delivery for ovarian cancer treatment.[27] Nevertheless, the use of non-degradable materials as drug carriers may significantly hamper its clinical utility.

Herein, we report LHRH-polysaccharide nanoparticles for targeted delivery of CDDP to breast tumor cells, utilizing carboxylic ligand functionalized dextran (dextran–succinic acid, Dex–SA) as the delivery carrier. Towards this aim, the carboxyl group modified polysaccharide Dex–SA was synthesized, then used to encapsulate CDDP in aqueous solution to form the micellar nanoparticles (Dex–SA–CDDP) of uniform size, and subsequently transformed into targeted nanoparticles (Dex–SA–CDDP–LHRH) by chemical conjugation of LHRH onto the surface of the Dex–SA–CDDP nanoparticles. Both the non-targeted and targeted nanoparticles displayed sustained drug release, prolonged blood circulation and excellent hemocompatibility. The targeting efficiency of the LHRH modified CDDP loaded micellar nanoparticles was evaluated in the aspects of cellular internalization and cytotoxicity by human breast cancer cells (MCF-7) *in vitro* and the tumor distribution and tumor suppression *in vivo*.

Experimental section

Materials

Dextran (Dex, 40 kDa) was purchased from Fluka and used without further purification. Succinic anhydride was obtained from Sinopharm Chemical Reagent Co., Ltd. Cisplatin (Shandong Boyuan Pharmaceutical Co., Ltd.), 4-dimethylaminopyridine (DMAP, Alfa Aesar), mercaptopropionic acid (Alfa Aesar), IR783 (Aldrich), 2,2′-(ethylenedioxy)bis(ethylamine) (Aldrich), 1-ethyl-(3-dimethylaminopropyl)carbodiimide hydrochloride (EDC·HCl, GL Biochem Ltd., Shanghai), *N*-hydroxysuccinimide (NHS, Fluka), 3-(4,5-dimethyl-thiazol-2-yl)-2,5-diphenyl tetrazolium bromide (MTT, Sigma) and a Micro BCA protein colorimetric assay kit (Thermo Scientific) were used as received. The LHRH peptide (Gln–His–Trp–Ser–Tyr–Lys–Leu–Arg–Pro–NHEt) was synthesized according to our design by ChinaPeptides Co. Ltd. IR783–S–COOH was prepared as described previously.[33] Dimethyl sulfoxide (DMSO) and dimethyl formamide (DMF) were stored over calcium hydride (CaH_2) and purified by vacuum distillation with CaH_2. Purified deionized water was prepared using a Milli-Q plus system (Millipore Co., Billerica, MA, USA).

Measurements

^1H and ^{13}C NMR spectra were recorded on a Bruker AV 400 NMR spectrometer in DMSO-d_6. Fourier transform infrared (FT-IR) spectra were recorded on a Bio-Rad Win-IR instrument using the KBr method. GPC analyses of Dex and Dex–SA were conducted on a Waters 2414 system equipped with an Ultrahydrogel™ linear column and a Waters 2414 refractive index detector (eluent: 0.1 M phosphate buffer, pH 7.4; flow rate: 0.5 mL min^{-1}; temperature: 35 °C; standard: poly(ethylene glycol)). Zeta potentials (ζ-potentials) of the samples were measured using a Zeta Potential/BI-90Plus particle size analyzer (Brookheaven Instruments Corporation, USA). Dynamic laser scattering (DLS) measurement was performed on a WyattQELS instrument with a vertically polarized He–Ne laser (DAWN EOS, Wyatt Technology, USA). The scattering angle was fixed at 90°. An inductively coupled plasma optical emission spectrometer (ICP-OES, iCAP 6300, Thermoscientific, USA) and an inductively coupled plasma mass spectrometer (ICP-MS, Xseries II, Thermoscientific, USA) were used for quantitative determination of platinum. A Thermo ESCALAB 250 X-ray photoelectron spectrometer was used for X-ray photoelectron spectroscopic (XPS) determination. Scanning transmission electron microscopy (STEM) images were recorded using a FEI TECNAI G2 20 high-resolution transmission electron microscope operating at 200 kV.

Preparation of Dex–SA–CDDP and Dex–SA–CDDP–LHRH nanoparticles

To prepare Dex–SA, dextran (5.002 g) was dissolved in 40 mL of dry DMSO and introduced into a flame-dried flask, followed by addition of 4-(dimethylamino)pyridine (1.878 g, 15.375 mmol) solution in DMSO (5.0 mL) and succinic anhydride (1.538 g, 15.375 mmol) in DMSO (5.0 mL), respectively. The reaction was performed at 30 °C for 48 h under nitrogen. The product was isolated by precipitation in cold ethanol, washed several times with ethanol, and dried under vacuum. The resulting white powder was then dissolved in deionized water, dialyzed against phosphate buffer (PB, 0.01 M, pH 7.0) and deionized water for 72 h to remove the excess reactants. The final product was obtained as a white powder after lyophilization of the dialyzed solution.

Dex–SA–CDDP nanoparticles were prepared by the complexation of Dex–SA with CDDP according to our previous protocol with minor modification.[26] Briefly, Dex–SA lyophilized powder (801.0 mg) was dissolved in 300.0 mL of deionized water, and then its pH was adjusted to 7.4 with a few drops of 0.05 M NaOH. Subsequently, 80.0 mg of CDDP was added into the polymer solution and the mixture solution was vigorously shaken at 37 °C for 72 h in the dark. The free CDDP was removed by dialysis (MWCO 7000) against deionized water for 24 h followed by lyophilization in the dark.

To prepare Dex–SA–CDDP–LHRH, 802.0 mg of Dex–SA was dissolved in 300.0 mL of deionized water and adjusted to pH 7.4 with NaOH. Then, 80.0 mg of CDDP was added and the resulting solution was vigorously shaken at 37 °C for 72 h in the dark. After dialysis against deionized water for 24 h, the resulting Dex–SA–CDDP nanoparticles were negatively charged and covered by carboxy groups. 1-Ethyl-(3-dimethylaminopropyl)-carbodiimide hydrochloride (32.3 mg) and *N*-hydroxysuccinimide (7.8 mg) were added into the Dex–SA–CDDP nanoparticle solution to activate carboxylic acid groups for 60 min, and then the LHRH peptide (42.0 mg) was added. The reaction was continued at 37 °C for 12 h. The free drug and other impurities were removed by dialysis as mentioned above. Then, the drug loaded nanoparticles were lyophilized for long-term storage.

IR783-labeled Dex–SA–CDDP and Dex–SA–CDDP–LHRH nanoparticles were prepared using a modified version of the method published by Ernsting *et al.*[34] Briefly, 2,2′-(ethylenedioxy)bis(ethylamine) (1.5 mg) was dissolved in deionized water (3.0 mL), to which IR783–S–COOH (8.3 mg), 1-ethyl-(3-dimethylaminopropyl)carbodiimide hydrochloride (2.3 mg) and *N*-hydroxysuccinimide (1.3 mg) were added. The solution was stirred for 12 h at room temperature and protected from light. Meanwhile, 30 mL of Dex–SA–CDDP or Dex–SA–CDDP–LHRH nanoparticles prepared using the methods mentioned above were transferred into a glass vial, followed by addition of 1-ethyl-(3-dimethylaminopropyl)carbodiimide hydrochloride (9.6 mg) and *N*-hydroxysuccinimide (2.3 mg) to activate carboxylic acid groups for 60 min. After being stirred for 12 h at room temperature, the amine-modified IR783 was covalently linked to Dex–SA–CDDP or Dex–SA–CDDP–LHRH nanoparticles with an activated carboxylate group by adding IR783 solution dropwise to Dex–SA–CDDP or Dex–SA–CDDP–LHRH solution. The mixture was stirred for another 12 h at room temperature, purified by dialysis for 24 h against deionized water, and then further purified by ultrafiltration (Millipore, MWCO, 100 kDa). A green powder was obtained after lyophilization.

The drug loading content (DLC) and drug loading efficiency (DLE) of CDDP were determined by using ICP-OES. DLC and DLE were calculated according to the following formula:

$$\text{DLC (wt\%)} = (\text{weight of loaded drug/weight of drug-loaded nanoparticles}) \times 100\%$$

$$\text{DLE (wt\%)} = (\text{weight of loaded drug/weight of feeding drug}) \times 100\%$$

The amount of LHRH conjugated on the surface of Dex–SA–CDDP–LHRH nanoparticles was measured using a Micro BCA Protein Assay Kit (Thermo Scientific), according to the manufacturer's instructions (free LHRH was used as the standard). The content of IR783 in the nanoparticles was determined by using a UV-vis spectrometer.

In vitro release of CDDP

To determine the release profiles of CDPP, the weighed freeze-dried CDDP-loaded nanoparticle powder was suspended in 5.0 mL of release medium and transferred into a dialysis bag (MWCO 3500 Da). The release experiment was initiated by placing the end-sealed dialysis bag into 50.0 mL of release medium at 37 °C with constant shaking. At selected time intervals, 3.0 mL of release media was taken out and replenished with an equal volume of fresh media. The amount of CDDP released was determined using ICP-MS. The release study of free CDDP was performed under the same conditions.

Cell cultures

The human breast cancer (MCF-7) cells were cultured at 37 °C in a 5% CO_2 atmosphere in Dulbecco's modified Eagle's medium (DMEM, Gibco) supplemented with 10% fetal bovine serum (FBS), penicillin (50 U mL^{-1}) and streptomycin (50 U mL^{-1}).

Cellular uptake and cytotoxicity assay

Briefly, MCF-7 cells were seeded in 6-well plates with a density of 3×10^5 cells per well in 2 mL of DMEM and incubated for 24 h, and then the original medium was replaced with free CDDP, Dex–SA–CDDP and Dex–SA–CDDP–LHRH (at a final CDDP concentration of 12.0 μM) containing DMEM. For the LHRH receptor blocking study, MCF-7 cancer cells were first incubated with free LHRH (20 μM) for 1 h, followed by co-incubation with Dex–SA–CDDP–LHRH. After incubation for 5 h at 37 °C, the cells were washed five times with phosphate buffered saline (PBS). The cells were trypsinized and cell numbers were counted. Then, the cells were digested with nitric acid (68 vol%) at 70 °C for 12 h. The platinum concentration was measured by ICP-MS.

The reported result of the sample is the average of three replicates.

The cytotoxicities of Dex–SA, free CDDP, Dex–SA–CDDP and Dex–SA–CDDP–LHRH were evaluated by MTT assay. The cells were seeded in 96-well plates (8×10^3 cells per well) in 100 μL of DMEM medium and incubated at 37 °C in a 5% CO_2 atmosphere for 24 h. The culture medium was replaced with 200 μL of fresh medium containing Dex–SA, free CDDP, Dex–SA– and Dex–SA–CDDP–LHRH. The cells were subjected to MTT assay after being incubated for another 24 h or 48 h. The absorbance of the solution was measured on a Bio-Rad 680 microplate reader at 490 nm. The relative cell viability was determined by comparing the absorbance at 490 nm with control wells containing only cell culture medium. Data are presented as means ± SD ($n = 6$).

Hemolysis assay

Hemolytic activity of Dex–SA, free CDDP, Dex–SA–CDDP and Dex–SA–CDDP–LHRH was evaluated according to a previous protocol.[35,36] PBS and triton X-100 (10 g L^{-1}), a surfactant known to lyse red blood cells (RBCs), were used as negative and positive controls, respectively. The hemolysis ratio (HR) of RBCs was calculated using the following formula: hemolysis (%) = $(A_{\text{sample}} - A_{\text{negative control}})/(A_{\text{positive control}} - A_{\text{negative control}}) \times 100$, where A_{sample}, $A_{\text{negative control}}$ and $A_{\text{positive control}}$ were denoted as the absorbance of samples, negative and positive controls, respectively. All hemolysis experiments were carried out in triplicate.

Pharmacokinetics

Wistar rats (250 ± 5 g) were randomly divided into three groups ($n = 3$). Free CDDP, Dex–SA–CDDP and Dex–SA–CDDP–LHRH were administered intravenously *via* tail vein (5 mg kg^{-1} CDDP). At defined time periods (1 min, 15 min, 30 min, 1 h, 2 h, 5 h, 8 h, 12 h, and 24 h), blood samples were collected from orbital cavity, heparinized, and centrifuged to obtain the plasma. The plasma samples were decomposed on heating in nitric acid and the platinum contents were measured by ICP-MS.

Ex vivo IR783 fluorescence imaging

The IR783 labeled Dex–SA–CDDP and Dex–SA–CDDP–LHRH nanoparticles were injected into MCF-7-tumor-bearing mice *via* lateral tail vein (5 mg kg^{-1} on IR783 basis). The mice were sacrificed 3 h post-injection. The tumor and major organs (heart, liver, spleen, lung and kidney) were excised, followed by washing the surface with physiological saline three times for *ex vivo* imaging of IR783 fluorescence using the Maestro *in vivo* Imaging System (Cambridge Research & Instrumentation, Inc., USA). The resulting data can be used to identify, separate, and remove the contribution of autofluorescence in analyzed images by the commercial software (Maestro 2.4). The average signals were also quantitatively analyzed using Maestro 2.4 software.

Orthotopic xenograft model and tumor suppression study

Female BALB/c nude mice were obtained from SLRC Laboratory Animal Company (Shanghai, China) and used at 6 weeks of age. All animals received care in compliance with the guidelines outlined in the Guide for the Care and Use of Laboratory Animals and all procedures were approved by the Animal Care and Use Committee of Jilin University. The xenograft tumor model was generated by the subcutaneous injection of MCF-7 cells (1.5×10^6) into the mammary fat pad of the mice. When the tumor volume was approximately 50 mm^3, mice were randomly divided into seven groups and then treated with PBS, CDDP (1.0 mg kg^{-1}), CDDP (4 mg kg^{-1}), Dex–SA–CDDP (4 mg kg^{-1} on CDDP basis), Dex–SA–CDDP (10 mg kg^{-1} on CDDP basis), Dex–SA–CDDP–LHRH (4 mg kg^{-1} on CDDP basis) and Dex–SA–CDDP–LHRH (10 mg kg^{-1} on CDDP basis) by intravenous injection on days 0, 4, and 8. The treatment efficacy and systemic toxicity were assessed by measuring the tumor volume and body weight, respectively. The tumor volume and tumor suppression rate were calculated by the following formulae:

$$\text{Tumor volume } (V) = a \times b^2/2$$

$$\text{Tumor suppression rate (TSR, \%)} = [(\bar{V}_c - \bar{V}_x)/\bar{V}_c)] \times 100\%$$

a and b are the longest and shortest diameters of the tumors measured using a vernier caliper. $\bar{V}$ is the average tumor volume. c represents the control group, while x represents the treatment group.

Results and discussion

Preparation and characterization of Dex–SA–CDDP and Dex–SA–CDDP–LHRH nanoparticles

Dextran is a United States Food and Drug Administration (FDA) approved material and has been used in a range of biomedical applications because of its excellent aqueous solubility, wide availability, biocompatibility, and ease of modification.[37,38] In this study, CDDP was encapsulated and targetedly delivered to breast cancer cells by Dex–SA polysaccharide nanoparticles surface-functionalized with LHRH peptides. As shown in Scheme 1, the synthesis procedures of CDDP-loaded LHRH-targeted nanoparticles involved (1) synthesis of Dex–SA by treating dextran with succinic anhydride in anhydrous DMSO, (2) preparation of CDDP loaded untargeted nanoparticles, and (3) conjugation of LHRH to the surface of Dex–SA–CDDP nanoparticles. This strategy facilitated the preparation of CDDP-loaded nanoparticles and guaranteed that the targeting molecules were conjugated on the surface of nanoparticles.

The actual degree of substitution (DS, defined as the number of SA units per 100 anhydroglucosidic units) of Dex–SA was determined to be 50 by ^{13}C NMR spectra (data not shown). The FT-IR spectrum of Dex–SA clearly revealed the presence of the absorbance peak at 1731 cm^{-1} characteristic of carboxyl moieties (data not shown). In comparison with that of dextran, the GPC trace of Dex–SA exhibited a clear shift to the higher M_n region (3.18×10^4 g mol^{-1}, $M_w/M_n = 1.82$), further indicating that the succinic acid was successfully grafted onto the dextran.

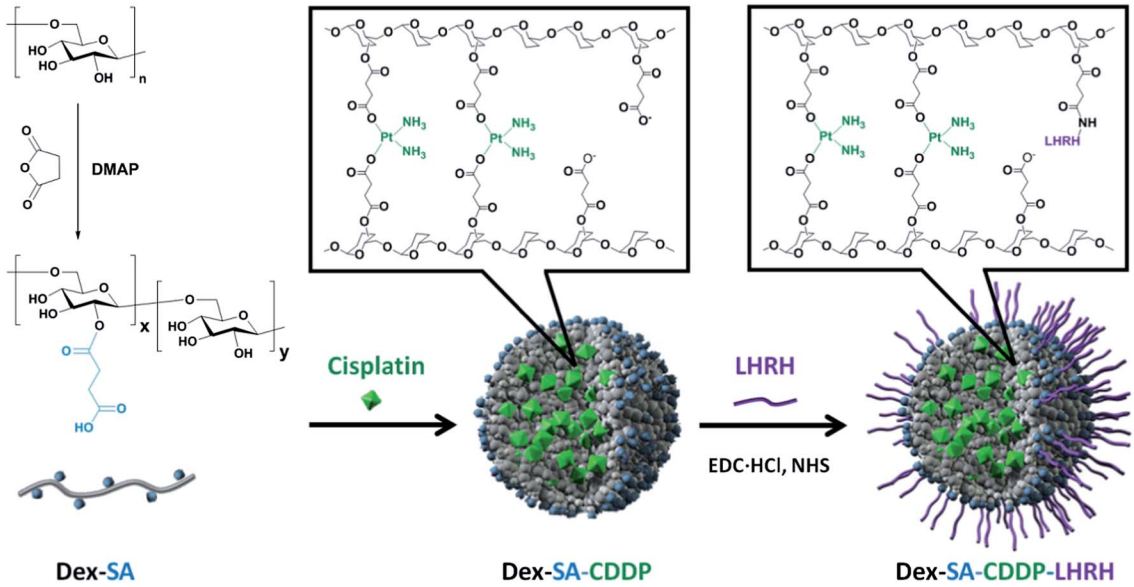

Scheme 1 The schematic illustration of the process of preparing Dex–SA, Dex–SA–CDDP and Dex–SA–CDDP–LHRH.

Dex–SA–CDDP nanoparticles with uniform size and narrow dispersion (Fig. 1A and C and Table 1, $D \approx 50$ nm by STEM and $R_h \approx 19$ nm by DLS) were easily obtained *via* chelate interactions between the ionic polymeric carrier and CDDP in aqueous solution. The results suggested that the Dex–SA–CDDP complex formed due to the substitution of two chlorides of CDDP by the carboxyl groups of Dex–SA.[7] To generate Dex–SA–CDDP–LHRH nanoparticles, LHRH peptides were chemically conjugated onto the surface of the Dex–SA–CDDP nanoparticles in the presence of EDC·HCl and NHS (Scheme 1). The particle size of Dex–SA–CDDP–LHRH increased modestly in comparison to Dex–SA–CDDP (Fig. 1B and C and Table 1, $D \approx 55$ nm by STEM and $R_h \approx 22$ nm by DLS), which can be attributed to the conjugation of LHRH on the nanoparticle surface. Moreover, the existence of LHRH peptides on the surface of Dex–SA–CDDP–LHRH was verified by XPS analysis. As shown in Fig. 1D and E, the signal intensity of N 1s at 400 eV increased after the conjugation of LHRH. The amount of LHRH on the nanoparticle surface was further quantified using the BCA protein assay, revealing a result of 45 μg peptide per mg of nanoparticles.

For both CDDP-loaded formulations, the binding energies at 75.8 and 72.2 eV were attributed to Pt $4f_{5/2}$ and Pt $4f_{7/2}$, respectively (Fig. 1F).[39] The binding energy of Pt $4f_{7/2}$ at 72.2 eV indicated the state of the platinum to be Pt(II).[39,40] The DLC and DLE of CDDP in Dex–SA–CDDP and Dex–SA–CDDP–LHRH nanoparticles were 8.1 and 7.5%, 88.3 and 85.5%, respectively, as detected by ICP-OES. Zeta-potential analyses demonstrated that both the targeted and non-targeted nanoparticles had negative surface charges, indicating good dispersion stability,[41] which would also minimize the undesirable rapid elimination of CDDP-loaded nanoparticles from the blood circulation, and facilitate their accumulation at the tumor sites.[42,43] Besides, it is worth noting that the surface charge of the Dex–SA–CDDP–LHRH nanoparticles increased from −19.7 to −16.8 mV after the conjugation of LHRH, revealing the consumption of the carboxylate groups by targeting molecules.

The *in vitro* release of CDDP from the Dex–SA–CDDP and Dex–SA–CDDP–LHRH nanoparticles was carried out in PBS at pH 7.4 by the dialysis method. As shown in Fig. 2, both CDDP-loaded formulations displayed a similar sustained release

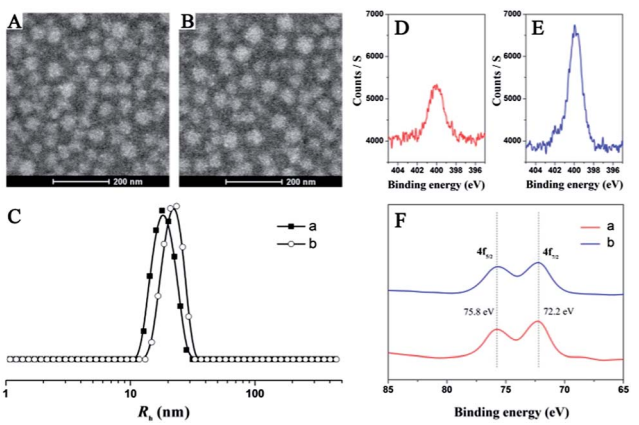

Fig. 1 (A and B) STEM images of (A) Dex–SA–CDDP and (B) Dex–SA–CDDP–LHRH. (C) Hydrodynamic radius distribution of (a) Dex–SA–CDDP and (b) Dex–SA–CDDP–LHRH. (D and E) XPS curves of N 1s in (D) Dex–SA–CDDP and (E) Dex–SA–CDDP–LHRH nanoparticles. (F) XPS curves of Pt 4f in (a) Dex–SA–CDDP and (b) Dex–SA–CDDP–LHRH nanoparticles.

Table 1 Characterization of the CDDP-loaded nanoparticles

Entry	DLC (%)	DLE (%)	Zeta potential (mV)	R_h (nm)
Dex–SA–CDDP	8.1	88.3	−19.7 ± 4.8	18.6 ± 6.3
Dex–SA–CDDP–LHRH	7.5	85.5	−16.8 ± 4.5	22.0 ± 7.1

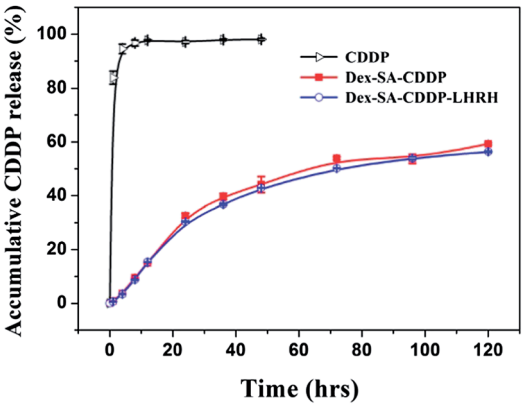

Fig. 2 *In vitro* drug release profiles of free CDDP, Dex–SA–CDDP and Dex–SA–CDDP–LHRH nanoparticles in PBS at 37 °C. Data represent the average values from triplicate experiments.

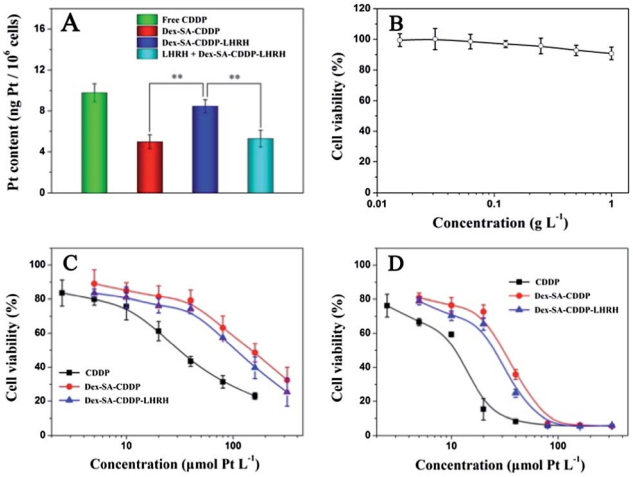

Fig. 3 (A) Platinum uptake in MCF-7 cells. The concentration of platinum in cells was determined after 5 h of incubation with medium containing CDDP or CDDP-loaded nanoparticles. (B) *In vitro* cytotoxicities of Dex–SA to MCF-7 cells after incubation for 48 h. (C and D) Cytotoxicities of CDDP, Dex–SA–CDDP and Dex–SA–CDDP–LHRH to MCF-7 cells after incubation for (C) 24 h and (D) 48 h.

profile without burst release (60% of the CDDP was released within 120 h), which indicated that the surface modification of nanoparticles with targeting ligands had no influence on drug retention. As a comparison, the release of free CDDP from dialysis bags was also investigated. A total release of more than 80% within the initial 1 h was observed for free CDDP. It was significantly faster than the drug release of CDDP-loaded nanoparticles. The release rate of free CDDP from the dialysis bags was consistent with the expected rate of diffusion for low molecular weight molecules across the dialysis membrane. This demonstrated that the dialysis membrane had less effect on the diffusion rate of CDDP, which was consistent with a previous study by Wooley *et al.*[15]

Cellular uptake and cytotoxicity study

To evaluate the biological activities of the ligand-linked nanoparticles, the cellular internalization in LHRH receptor-positive MCF-7 cells was quantitatively analyzed by ICP-MS.[44,45]

As shown in Fig. 3A, the intracellular platinum content was significantly higher in Dex–SA–CDDP–LHRH-treated cells (8.45 ng Pt per 10^6 cells) than in cells treated with Dex–SA–CDDP nanoparticles (4.97 ng Pt per 10^6 cells, $P < 0.01$) or Dex–SA–CDDP–LHRH nanoparticles plus free LHRH (5.28 ng Pt per 10^6 cells, $P < 0.01$) after 5 h incubation, suggesting that the LHRH-functionalized nanoparticles were recognized by LHRH receptors on the surface of breast cancer cells and internalized through receptor-mediated endocytosis.[46] Nevertheless, the intracellular platinum content in the Dex–SA–CDDP–LHRH group was still lower than that in the free CDDP group (9.78 ng Pt per 10^6 cells). This might be explained by the negative surface charge, which would repel the anionic nanoparticles on the cell surface, and subsequently prevent cellular uptake.[35,47] On the other hand, free CDDP was speculated to enter the cells *via* passive diffusion, while the CDDP-loaded nanoparticles were most likely to be internalized *via* a slower endocytosis pathway.[7,8]

Next, the cytotoxicity of Dex–SA, Dex–SA–CDDP and Dex–SA–CDDP–LHRH was examined by the MTT assay. The biocompatibility studies using MCF-7 cells revealed that Dex–SA was nontoxic up to the highest testing concentration of 1 g L^{-1} (Fig. 3B), indicating its excellent biocompatibility. It could be observed from Fig. 3C and D that all CDDP formulations demonstrated dose and time dependent toxicity toward MCF-7 cells. Consistent with the previous reports, the cytotoxicity of CDDP was significantly decreased after its incorporation into the polysaccharide nanoparticles. This could be attributed to the slower internalization of the CDDP-loaded nanoparticles into cells and slow release of the encapsulated drug from the carriers.[27] It should be noted that the introduction of LHRH ligands increased the *in vitro* cytotoxicity of Dex–SA–CDDP nanoparticles. The results obtained 24 h after incubation showed that the 50% growth inhibitory concentration (IC50) of Dex–SA–CDDP–LHRH was 106.3 μmol Pt L^{-1}, which was lower than that of Dex–SA–CDDP (146.4 μmol Pt L^{-1}). But this gap was narrowed when the incubation time was extended to 48 h (25.5 μmol Pt L^{-1} *versus* 31.0 μmol Pt L^{-1}). These data suggest that the LHRH peptide provided not only enhanced accumulation of CDDP-loaded targeted nanoparticles in the receptor-positive cells but also increased cytotoxicity of these nanoparticles.

Hemolysis and pharmacokinetics

Hemolysis assays are generally considered valuable in testing the hemocompatibility of a drug formulation.[48] In this study, a hemolysis assay was carried out based on the previous report.[36] As shown in Fig. 4A–C, both Dex–SA and the CDDP-loaded nanoparticles showed negligible hemolysis toxicity (~0%) to RBCs at all concentrations tested, demonstrating the excellent blood compatibility of the CDDP-loaded nanoparticles and the potential application as a drug delivery system for intravenous injection.

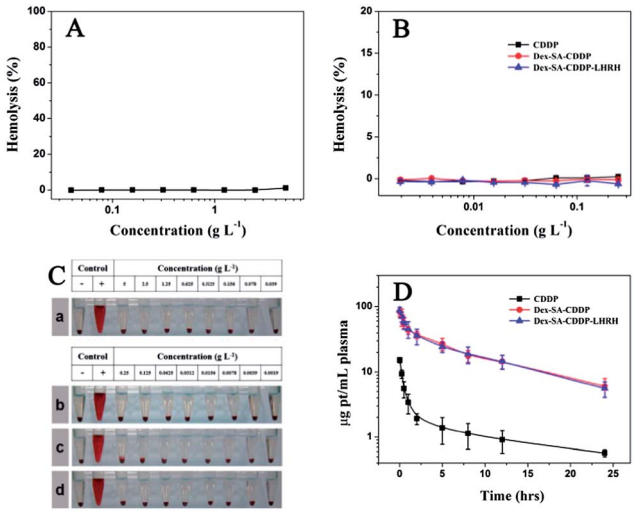

Fig. 4 (A) Hemolytic activity of Dex–SA. (B) Hemolytic activity of CDDP, Dex–SA–CDDP and Dex–SA–CDDP–LHRH. (C) Photographs of hemolysis of RBCs after the treatment with (a) Dex–SA, (b) CDDP, (c) Dex–SA–CDDP and (d) Dex–SA–CDDP–LHRH. The red hemoglobin in the supernatant indicates the damage to RBCs. Triton X-100 and PBS are used as positive (+) and negative (−) controls, respectively. (D) *In vivo* pharmacokinetic profiles after intravenous injection of CDDP, Dex–SA–CDDP and Dex–SA–CDDP–LHRH in rats. Data are presented as mean ± standard deviation ($n = 3$).

Most of the small molecule anticancer drugs currently in clinical use, including cisplatin, doxorubicin, gemcitabine and paclitaxel, are inherently associated with the lack of tumor selectivity and a short blood circulation time, which cause an unsatisfactory therapeutic effect and various toxic side effects.[6,49] Previous studies have demonstrated that 65 to 98% of cisplatin is bound to blood plasma proteins, and most of the platinum (50–61%) from cisplatin added to human blood plasma at physiologically relevant doses is bound to albumin.[50] A significantly prolonged blood circulation time and reduced chelation of cisplatin to plasma proteins could be achieved after the encapsulation of cisplatin in the form of a prodrug.[6,26]

The plasma platinum levels after intravenous injection of free CDDP and CDDP-incorporated nanoparticles are shown in Fig. 4D. Both the targeted and non-targeted CDDP-incorporated nanoparticles showed remarkably prolonged blood circulation, with more than 7% left in 24 h, whereas free CDDP underwent an instant platinum concentration decrease after the administration, with less than 3% in the plasma 2 h after injection. The improved blood retention time of the CDDP incorporated nanoparticles was reasonably correlated with the inherent enhanced retention effect of the uniform nanoparticles bearing slightly negative charges and the delayed drug release behavior during blood circulation. Thus long circulation and sustained drug release behavior of the CDDP-loaded nanoparticles would contribute to the increased accumulation at the tumor site through the EPR effect and reduced systemic toxicity.

Biodistribution and *in vivo* anticancer efficacy

Generally, the tumor-targeted drug delivery process following systemic administration can be divided into four stages,[42,51] as shown in Scheme 2: (1) the drug-loaded nanoparticles circulate in the bloodstream; (2) the drug-loaded nanocarriers accumulate in the tumor *via* the EPR effect and further penetrate into the deep tumor tissue; (3) the drug-encapsulated vehicles enter the tumor cells *via* one or several possible pathways; and (4) the vehicles release the drug cargo and kill the malignant cells.

To evaluate the effects of CDDP-loaded LHRH-conjugated targeted and non-targeted nanoparticles on the *in vivo* biodistribution of CDDP, a small-molecular near-infrared fluorescent probe (IR783) was conjugated to the nanoparticles, and *ex vivo* imaging of the major organs and tumors 3 h

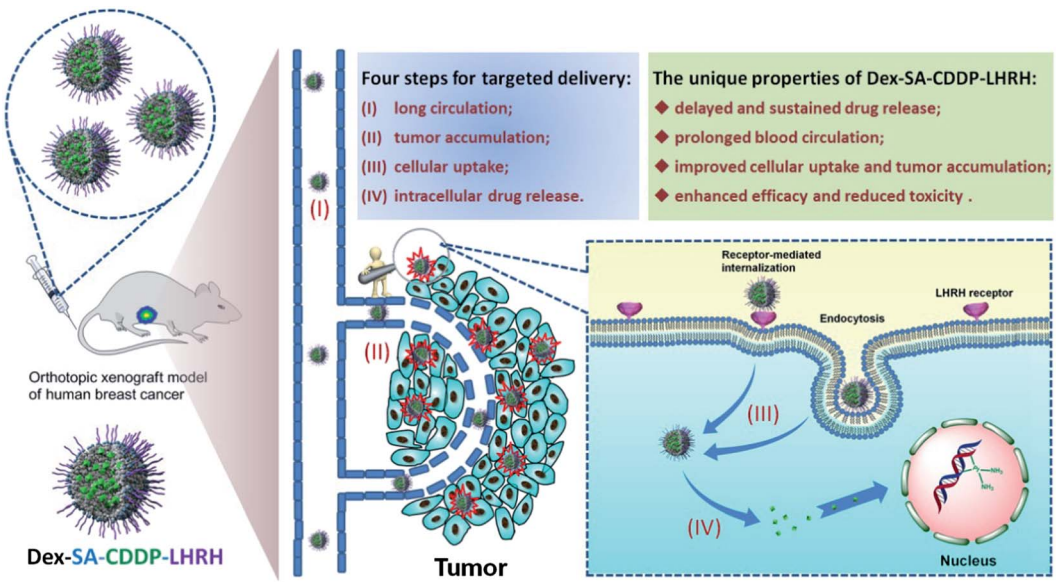

Scheme 2 The schematic illustration of the intravenous injection, blood circulation, tumor accumulation, cellular uptake and intracellular drug release of Dex–SA–CDDP–LHRH nanoparticles.

post-injection was carried out in nude mice bearing MCF-7 tumors. The fluorescence intensity of IR783 is represented in Fig. 5A in terms of a color scale and semi-quantitatively analyzed in Fig. 5B.

As a control, no fluorescence was observed in the major organs and tumor for mouse treated with PBS. Most of the CDDP-loaded non-targeted nanoparticles were accumulated in the liver, and their contents in the heart, spleen, lung, kidney, and tumor tissue were relatively lower, implicating that the CDDP-loaded polysaccharide nanoparticles as foreign bodies were mainly captured and metabolized by the liver.[52–54] The fluorescence intensity of the non-targeted nanoparticles in tumor tissues was slightly stronger than those in the kidney and lung that are well-known clearing and metabolic organs. This could be attributed to the prolonged blood circulation and EPR effect of the tumor. Notably, the LHRH-targeted nanoparticles did not obviously alter the distribution in the normal organs including heart, liver, spleen, lung and kidney. However, the fluorescence intensity of Dex–SA–CDDP–LHRH in the tumors was around 2-fold higher than that of Dex–SA–CDDP (Fig. 5B). Together, these findings demonstrated the tumor-selective targeted delivery of CDDP using LHRH-functionalized nanoparticles.

Based on the appropriate physicochemical properties, sustained drug release behavior, prolonged blood circulation and enhanced tumor localization, the CDDP-loaded LHRH-targeted nanoparticles might contribute to superior antitumor efficacy without unexpected side effects. To provide *in vivo* evidence for the antitumor potential of Dex–SA–CDDP–LHRH, the antitumor efficacy was further investigated on BALB-c/nude mice bearing human breast tumors (MCF-7). The treatments were done by intravenously injecting PBS, CDDP (1 mg kg^{-1}), CDDP (4 mg kg^{-1}), Dex–SA–CDDP (4 mg kg^{-1} CDDP eq.), Dex–SA–CDDP (10 mg kg^{-1} CDDP eq.), Dex–SA–CDDP–LHRH (4 mg kg^{-1} CDDP eq.), and Dex–SA–CDDP–LHRH (10 mg kg^{-1} CDDP eq.), respectively, into tumor-bearing mice.

As shown in Fig. 6A, both free CDDP and CDDP-loaded nanoparticle formulations could retard tumor growth compared to the control group (treated with PBS) in a dose-dependent manner.

Free CDDP at a low dose of 1 mg kg^{-1} could not effectively inhibit the tumor growth. An enhanced anti-tumor efficacy was observed when the CDDP dosage was increased to 4 mg kg^{-1}. At day 16 post-injection, the average tumor volumes of free CDDP (1 mg kg^{-1}) and free CDDP (4 mg kg^{-1}) were 82.9% and 53.1% of that in the control group. The non-targeted nanoparticles displayed a weak suppression of tumor growth at an equivalent CDDP dose of 4 mg kg^{-1}. In contrast, the LHRH-targeted nanoparticles exhibited a decreased tumor volume compared to CDDP at a dose of 4 mg kg^{-1} during the treatment. Further increasing the drug dosage of CDDP-encapsulated nanoparticles to 10 mg kg^{-1} resulted in enhanced tumor growth suppression. The most efficient inhibition of tumor growth was observed in the Dex–SA–CDDP–LHRH treated group at a dose of 10 mg kg^{-1}, with the highest tumor suppression rate of 70.4% after 16 days (Fig. 6C).

Body weight change was simultaneously monitored and is shown in Fig. 6B, where the body weight on day 0 is normalized to 100%. Mice receiving PBS, Dex–SA–CDDP (4 mg kg^{-1} CDDP) and Dex–SA–CDDP–LHRH (4 mg kg^{-1} CDDP) showed almost no difference in the physical activity level and body weight after 16 days, indicating that CDDP-encapsulated nanoparticles were well tolerated at a dose of 4 mg kg^{-1}. Mice treated with free CDDP at a dose of 1 mg kg^{-1} exhibited a stable body weight for the first 8 days, followed by a continuous body weight loss after the last treatment. Evident dose dependent systemic toxicity could be found, when free CDDP at a dose of 1 mg kg^{-1} and 4 mg kg^{-1} was compared. Treatment of free CDDP at a dose of 4 mg kg^{-1} resulted in a significant loss of body weight, with about 26% weight loss by the 16th day after the first treatment. Both the CDDP-loaded targeted and non-targeted nanoparticles at a higher dose of 10 mg kg^{-1} induced body weight loss for the first 10 days and gradual recovery thereafter. Thus, the CDDP-loaded nano-sized drug delivery system could significantly reduce systemic toxicity of CDDP, at the doses and schedules of administration used in the present study.

These results indicated that Dex–SA–CDDP–LHRH was an effective and safe enough drug formulation for the xenograft MCF-7 cancer tumor model. In addition, there is significant potential in the application of Dex–SA–CDDP–LHRH in targeted delivery of CDDP for the treatment of ovarian, prostate and lung cancers which are known for LHRH overexpression.[30,31,55]

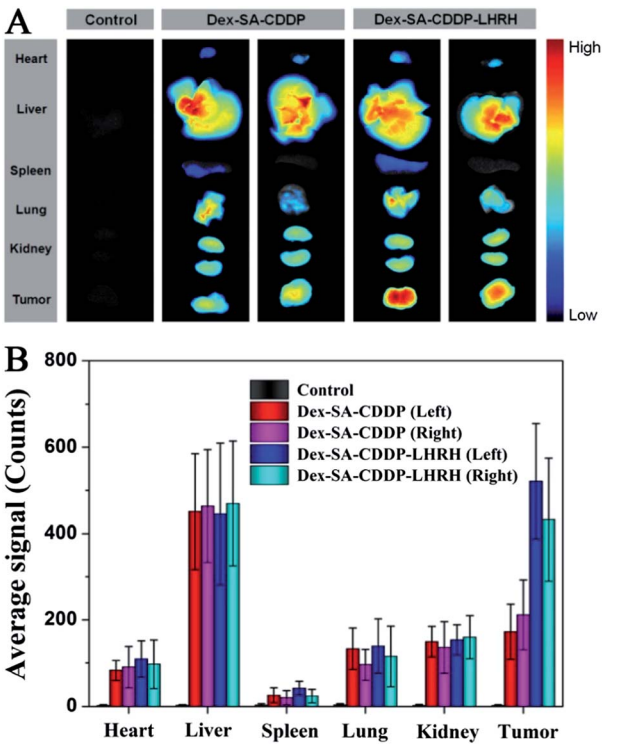

Fig. 5 Biodistribution of IR783 labeled Dex–SA–CDDP and Dex–SA–CDDP–LHRH in nude mice bearing MCF-7 tumor. (A) *Ex vivo* imaging of the major organs (heart, liver, spleen, lung and kidney) and tumors harvested 3 h post-injection. Mouse treated with PBS was used as a control. (B) Average signals collected from the major organs and tumors.

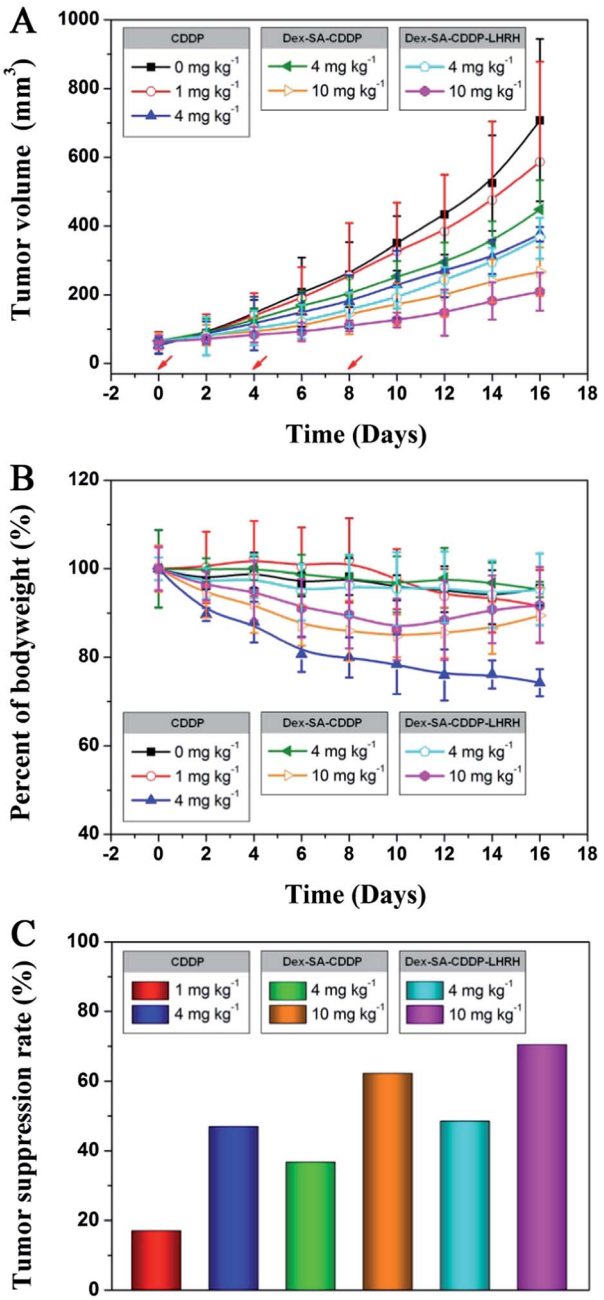

Fig. 6 (A) Tumor volume of established MCF-7 xenografts in BALB/c mice that received different treatments as indicated. The arrows represent the day on which the intravenous tail vein injection was performed. Data are presented as mean ± standard deviation ($n = 6$). (B) Body weight changes with the time of tumor-bearing mice. (C) Tumor suppression degree on the 16th day.

Conclusions

In the present investigation, the dextran-based nanoparticles for CDDP delivery to breast cancer cells were developed. Both the non-targeted and targeted nanoparticles could significantly prolong the blood circulation of CDDP and reduce the systemic toxicity attributed to the delayed and sustained drug release behavior. Importantly, the LHRH-targeted nanoparticles led to significant higher drug internalization in MCF-7 tumor cells *in vitro* and enhanced accumulation in MCF-7 xenograft tumors *in vivo*, compared with the non-targeted counterparts. Furthermore, systemic delivery of the targeted nanoparticles carrying CDDP *via* intravenous injection could significantly delay tumor growth in MCF-7 tumor bearing mice compared to the non-targeted nanoparticles and free CDDP at 4 mg kg^{-1}, probably due to its prolonged blood circulation and enhanced drug accumulation by active targeted delivery. An enhanced anti-tumor efficacy with moderate weight loss could be achieved, when the drug dosage of CDDP-encapsulated nanoparticles was increased to 10 mg kg^{-1}. Since CDDP has been widely used in clinical applications for many years, and dextran and succinic acid have been proven by FDA for parenteral use, our novel nanoparticle delivery system has great potential to be used in the clinic for targeted cancer treatment in the future.

Acknowledgements

This research was financially supported by the National Natural Science Foundation of China (projects 51173184, 51373168, 51390484, 51233004 and 51321062), the Ministry of Science and Technology of China (International Cooperation and Communication Program 2011DFR51090) and the Program of Scientific Development of Jilin Province (20130727050YY, 20130521011JH and 20130206066GX).

Notes and references

1 F. P. Seib and D. L. Kaplan, *Biomaterials*, 2012, **33**, 8442–8450.
2 A. L. Laine, E. Adriaenssens, A. Vessieres, G. Jaouen, C. Corbet, E. Desruelles, P. Pigeon, R. A. Toillon and C. Passirani, *Biomaterials*, 2013, **34**, 6949–6956.
3 X. Ma, J. Zhou, C. X. Zhang, X. Y. Li, N. Li, R. J. Ju, J. F. Shi, M. G. Sun, W. Y. Zhao, L. M. Mu, Y. Yan and W. L. Lu, *Biomaterials*, 2013, **34**, 4452–4465.
4 H. F. Ye, L. Jin, R. Z. Hu, Z. F. Yi, J. Li, Y. L. Wu, X. G. Xuguang and Z. R. Wu, *Biomaterials*, 2006, **27**, 5958–5965.
5 R. Wang, X. L. Hu, H. H. Xiao, Z. G. Xie, Y. B. Huang and X. B. Jing, *J. Mater. Chem. B*, 2013, **1**, 744–748.
6 S. Dhar, N. Kolishetti, S. J. Lippard and O. C. Farokhzad, *Proc. Natl. Acad. Sci. U. S. A.*, 2011, **108**, 1850–1855.
7 X. H. Peng, Y. Wang, D. Huang, Y. Wang, H. J. Shin, Z. Chen, M. B. Spewak, H. Mao, X. Wang, Y. Wang, Z. G. Chen, S. Nie and D. M. Shin, *ACS Nano*, 2011, **5**, 9480–9493.
8 M. Q. Li, Z. H. Tang, H. Sun, J. X. Ding, W. T. Song and X. S. Chen, *Polym. Chem.*, 2013, **4**, 1199–1207.
9 Y.-C. Wang, Y. Li, T.-M. Sun, M.-H. Xiong, J. Wu, Y.-Y. Yang and J. Wang, *Macromol. Rapid Commun.*, 2010, **31**, 1201–1206.
10 Y. Kuang, J. Liu, Z. Liu and R. Zhuo, *Biomaterials*, 2012, **33**, 1596–1606.
11 S. Guo, Y. Wang, L. Miao, Z. Xu, C. M. Lin, Y. Zhang and L. Huang, *ACS Nano*, 2013, **7**, 9896–9904.
12 T. Kapp, A. Dullin and R. Gust, *Bioconjugate Chem.*, 2010, **21**, 328–337.

13 S. D. Li and S. B. Howell, *Mol. Pharm.*, 2010, **7**, 280–290.
14 V. T. Huynh, J. Y. Quek, P. L. de Souza and M. H. Stenzel, *Biomacromolecules*, 2012, **13**, 1010–1023.
15 F. Zhang, M. Elsabahy, S. Zhang, L. Y. Lin, J. Zou and K. L. Wooley, *Nanoscale*, 2013, **5**, 3220–3225.
16 N. Nishiyama, S. Okazaki, H. Cabral, M. Miyamoto, Y. Kato, Y. Sugiyama, K. Nishio, Y. Matsumura and K. Kataoka, *Cancer Res.*, 2003, **63**, 8977–8983.
17 R. Plummer, R. H. Wilson, H. Calvert, A. V. Boddy, M. Griffin, J. Sludden, M. J. Tilby, M. Eatock, D. G. Pearson, C. J. Ottley, Y. Matsumura, K. Kataoka and T. Nishiya, *Br. J. Cancer*, 2011, **104**, 593–598.
18 C. Deng, Y. Jiang, R. Cheng, F. Meng and Z. Zhong, *Nano Today*, 2012, **7**, 467–480.
19 E. Wexselblatt, E. Yavin and D. Gibson, *Angew. Chem., Int. Ed.*, 2013, **52**, 6059–6062.
20 Y. Min, C. Q. Mao, S. Chen, G. Ma, J. Wang and Y. Liu, *Angew. Chem., Int. Ed.*, 2012, **51**, 6742–6747.
21 H. H. Xiao, H. Q. Song, Q. Yang, H. D. Cai, R. G. Qi, L. S. Yan, S. Liu, Y. H. Zheng, Y. B. Huang, T. J. Liu and X. B. Jing, *Biomaterials*, 2012, **33**, 6507–6519.
22 H. Q. Song, H. H. Xiao, Y. Zhang, H. D. Cai, R. Wang, Y. H. Zheng, Y. B. Huang, Y. X. Li, Z. G. Xie, T. J. Liu and X. B. Jing, *J. Mater. Chem. B*, 2013, **1**, 762–772.
23 B. Ahn, J. Park, K. Singha, H. Park and W. J. Kim, *J. Mater. Chem. B*, 2013, **1**, 2829–2836.
24 J. Nicolas, S. Mura, D. Brambilla, N. Mackiewicz and P. Couvreur, *Chem. Soc. Rev.*, 2013, **42**, 1147–1235.
25 Y. Miura, T. Takenaka, K. Toh, S. Wu, H. Nishihara, M. R. Kano, Y. Ino, T. Nomoto, Y. Matsumoto, H. Koyama, H. Cabral, N. Nishiyama and K. Kataoka, *ACS Nano*, 2013, **7**, 8583–8592.
26 W. Song, M. Li, Z. Tang, Q. Li, Y. Yang, H. Liu, T. Duan, H. Hong and X. Chen, *Macromol. Biosci.*, 2012, **12**, 1514–1523.
27 N. V. Nukolova, H. S. Oberoi, Y. Zhao, V. P. Chekhonin, A. V. Kabanov and T. K. Bronich, *Mol. Pharm.*, 2013, **10**, 3913–3921.
28 R. Wang, X. L. Hu, J. Yue, W. J. Zhang, L. Y. Cai, Z. G. Xie, Y. B. Huang and X. B. Jing, *J. Mater. Chem. B*, 2013, **1**, 293–301.
29 N. Wiradharma, Y. Zhang, S. Venkataraman, J. L. Hedrick and Y. Y. Yang, *Nano Today*, 2009, **4**, 302–317.
30 S. S. Dharap, Y. Wang, P. Chandna, J. J. Khandare, B. Qiu, S. Gunaseelan, P. J. Sinko, S. Stein, A. Farmanfarmaian and T. Minko, *Proc. Natl. Acad. Sci. U. S. A.*, 2005, **102**, 12962–12967.
31 M. Saad, O. B. Garbuzenko, E. Ber, P. Chandna, J. J. Khandare, V. P. Pozharov and T. Minko, *J. Controlled Release*, 2008, **130**, 107–114.
32 A. Taheri, R. Dinarvand, F. Ahadi, M. R. Khorramizadeh and F. Atyabi, *Int. J. Pharm.*, 2012, **431**, 183–189.
33 C. Li, K. Li, H. Yan, G. Li, J. Xia and X. Wei, *Chem. Commun.*, 2010, **46**, 1326–1328.
34 M. J. Ernsting, W.-L. Tang, N. MacCallum and S.-D. Li, *Bioconjugate Chem.*, 2011, **22**, 2474–2486.
35 M. Li, W. Song, Z. Tang, S. Lv, L. Lin, H. Sun, Q. Li, Y. Yang, H. Hong and X. Chen, *ACS Appl. Mater. Interfaces*, 2013, **5**, 1781–1792.
36 J. Ding, C. Xiao, Y. Li, Y. Cheng, N. Wang, C. He, X. Zhuang, X. Zhu and X. Chen, *J. Controlled Release*, 2013, **169**, 193–203.
37 Y.-L. Li, L. Zhu, Z. Liu, R. Cheng, F. Meng, J.-H. Cui, S.-J. Ji and Z. Zhong, *Angew. Chem., Int. Ed.*, 2009, **48**, 9914–9918.
38 N. Kanthamneni, S. Sharma, S. A. Meenach, B. Billet, J. C. Zhao, E. M. Bachelder and K. M. Ainslie, *Int. J. Pharm.*, 2012, **431**, 101–110.
39 C. Huang, K. G. Neoh, L. Xu, E. T. Kang and E. Chiong, *Biomacromolecules*, 2012, **13**, 2513–2520.
40 H. H. Xiao, D. F. Zhou, S. Liu, Y. H. Zheng, Y. B. Huang and X. B. Jing, *Acta Biomater.*, 2012, **8**, 1859–1868.
41 Z. Wang, Y. Yu, W. Dai, J. Lu, J. Cui, H. Wu, L. Yuan, H. Zhang, X. Wang, J. Wang, X. Zhang and Q. Zhang, *Biomaterials*, 2012, **33**, 8451–8460.
42 X. Z. Yang, X. J. Du, Y. Liu, Y. H. Zhu, Y. Z. Liu, Y. P. Li and J. Wang, *Adv. Mater.*, 2014, **26**, 931–936.
43 M. Ding, N. Song, X. He, J. Li, L. Zhou, H. Tan, Q. Fu and Q. Gu, *ACS Nano*, 2013, **7**, 1918–1928.
44 Y. N. He, L. H. Zhang and C. X. Song, *J. Controlled Release*, 2011, **152**, E29–E31.
45 S. S. Dharap and T. Minko, *Pharm. Res.*, 2003, **20**, 889–896.
46 X. Jiang, X. Sha, H. Xin, X. Xu, J. Gu, W. Xia, S. Chen, Y. Xie, L. Chen, Y. Chen and X. Fang, *Biomaterials*, 2013, **34**, 2969–2979.
47 C. Freese, M. I. Gibson, H.-A. Klok, R. E. Unger and C. J. Kirkpatrick, *Biomacromolecules*, 2012, **13**, 1533–1543.
48 B. Naeye, H. Deschout, M. Röding, M. Rudemo, J. Delanghe, K. Devreese, J. Demeester, K. Braeckmans, S. C. De Smedt and K. Raemdonck, *Biomaterials*, 2011, **32**, 9120–9127.
49 S. Lv, M. Li, Z. Tang, W. Song, H. Sun, H. Liu and X. Chen, *Acta Biomater.*, 2013, **9**, 9330–9342.
50 W. Hu, Q. Luo, K. Wu, X. Li, F. Wang, Y. Chen, X. Ma, J. Wang, J. Liu, S. Xiong and P. J. Sadler, *Chem. Commun.*, 2011, **47**, 6006–6008.
51 Q. Sun, M. Radosz and Y. Shen, *J. Controlled Release*, 2012, **164**, 156–169.
52 P. A. Ma, S. Liu, Y. B. Huang, X. S. Chen, L. P. Zhang and X. B. Jing, *Biomaterials*, 2010, **31**, 2646–2654.
53 M. Li, S. Lv, Z. Tang, W. Song, H. Yu, H. Sun, H. Liu and X. Chen, *Macromol. Biosci.*, 2013, **13**, 1150–1162.
54 L. Z. Zhang, Y. J. Zhang, W. Wu and X. Q. Jiang, *Chin. J. Polym. Sci.*, 2013, **31**, 778–786.
55 C. Yates, S. Sharp, J. Jones, D. Topps, M. Coleman, R. Aneja, J. Jaynes and T. Turner, *Biochem. Pharmacol.*, 2011, **81**, 104–110.